Journal of the Civil Engineering Forum, September 2025, 11(3):285-296
DOI 10.22146/jcef.21159
Available Online at https://jurnal.ugm.ac.id/v3/jcef/issue/archive

Seismic Performance of Reinforced Concrete Buildings in Darchula, Nepal: A Fragility-Based Approach

Birendra Kumar Bohara[1*], Benbokhari Abdellatif[2], Jyoti Deupa[1], Nirmal Mani Joshi[3], Sangam Jagari[3]
[1]Assistant Professor, School of Engineering, Far Western University, Kanchanpur-10400, NEPAL
[2]Laboratoire LTPiTE, Ecole Nationale Supérieure des Travaux Publics, ALGERIA
[3]School of Engineering, Far Western University, Mahendranagar, Kanchanpur-10400, NEPAL
*Corresponding author: birendra.bohara@fwu.edu.np

SUBMITTED 30 April 2025 **REVISED** 27 June 2025 **ACCEPTED** 30 June 2025

ABSTRACT This research evaluated the seismic vulnerability of non-engineered reinforced concrete (RC) buildings compared with that of engineered RC structures in the Darchula region of Far-Western Nepal, an area prone to high seismic risk. This study emphasizes the seismic performance of buildings under various loading conditions by examining construction practices and identifying structural deficiencies in RC buildings in Darchula, Nepal. Linear elastic and nonlinear pushover analyses are used to assess periods, mass participation, base shear, inter-story drift, capacity curves, nonlinear drift demand, and fragility curves. Models designed according to national and international standards are compared with non-engineered buildings (S1 – S6) to highlight the discrepancies in seismic resilience. The study further provides a probabilistic fragility framework to quantify damage likelihood at varying seismic demand levels. The results show that engineered buildings exhibit significantly greater resistance to seismic forces, with greater flexibility and higher base shear capacities. In contrast, non-engineered buildings, particularly shorter structures, are more prone to damage under moderate seismic events. Research indicates that ground floors in non-engineered buildings consistently exhibit the most significant inter-story drift as a result of soft-story impacts, highlighting them as crucial failure points. Fragility curves derived from spectral displacement values reveal that non-engineered buildings reach critical damage states at lower levels of seismic demand, indicating greater vulnerability. This research underscores the importance of enforcing seismic design standards and retrofitting non-engineered buildings to improve their earthquake resilience in seismic hotspots such as Darchula, Nepal. These findings provide a foundation for future seismic risk reduction strategies and highlight the urgent need for improved building practices to mitigate earthquake-related damage.

KEYWORDS Engineered buildings, Non-engineered Buildings, Seismic vulnerability, Pushover analysis, Fragility curve, Darchula

1 INTRODUCTION

Nepal is situated in the seismically active Himalayan – Hindukush region, where the convergence of the Indian and Eurasian tectonic plates results in a high risk of earthquakes. This area is notable for its intricate seismotectonic conditions, regular seismic activity, and geological instability, with some of the most catastrophic earthquakes (Chaulagain et al., 2018). The country's susceptibility is amplified by various fault systems, including the Himalayan megathrust fault, which significantly shapes its geological and topographical characteristics (Parajuli et al., 2021). Nepal's seismic past is marked by severe incidents such as the Nepal-Bihar earthquake (1934), Gorkha earthquake (2015), and the Jajarkot earthquake in the western region (Poudel and Chaulagain, 2024). These disasters have caused extensive loss of life and widespread damage, exposing significant shortcomings in structural resilience, especially in non-engineered and inadequately constructed buildings (Bhagat et al., 2018).

In Nepal, especially in western areas such as Darchula, Achham, and Dadeldhura, evaluating seismic risk is essential for protecting lives and shaping policies aimed at risk reduction and structural resilience. These regions, which are characterized by mountainous terrain and regular seismic occurrences resulting from the Himalayan megathrust fault, are vulnerable because of substandard construction practices and poor adherence to modern building regulations (Bohara, 2023; Poudel and Chaulagain, 2024). Darchula district lies in a highly seismically active zone due to its proximity to the main Himalayan thrust fault system. According to the recent study (Maharjan et al., 2023) and Indian Standard IS 1893:2016 (Bureau of Indian Standards, 2016), Darchula falls within Seismic Zone V, which is assigned a zone factor (Z) of 0.36, the highest seismic classification, indicating potential for very severe ground shaking.

Despite Nepal's high seismic risk, there is a lack of studies focusing on the seismic vulnerability of non-engineered reinforced concrete (RC) structures in Darchula. Limited field-based modeling and fragility assessments exist for this region, highlighting the need

for localized seismic analysis to inform risk mitigation strategies. When both analytical and empirical methodologies are used to assess seismic vulnerability, Nepal might benefit from the use of comparable strategies, including mechanical modeling to analyze its building inventory. Implementing advanced techniques such as deriving fragility curves through displacement-based or capacity spectrum methods could improve the comprehension of structural behavior under seismic forces (Gondaliya et al., 2025).

1.1 Objectives of the Study

The primary objective of this research is to assess the seismic vulnerability of RC structures in Far-Western Nepal, with a particular focus on non-engineered and inadequately designed structures in the Darchula district. To achieve this, the study pursues the following specific objectives:

1. Evaluate the seismic vulnerability of the RC buildings in Darchula using nonlinear static analysis and fragility-based analysis.
2. Develop lognormal fragility curves for different types of RC building based on design standards and construction periods.
3. Classify the likelihood of damage in various types of RC building under seismic loading conditions.
4. Identify high-risk RC building types.

2 METHODOLOGY

The overall methodology adopted in this study is illustrated in Figure 1, which outlines the sequential process from field survey and model development to seismic analysis and fragility assessment.

2.1 Modelling of Common Construction Practices for RC Buildings

Based on the surveyed data, three-story RC buildings, which are typically constructed in Darchula, are selected. The spacing of the bays, story height, seismic property, material property, size of the columns, and story of the buildings were selected based on the observations of the buildings as shown in Table 1. The plan and three-dimensional view of the studied buildings can be seen in Figures 2 and 3. Eight types of models of RC buildings are used in the study, in which the beam and column sizes of the buildings are changed based on the data obtained in the surveys. Table 2 shows the 9 models with different column beams and the area of rebar used in the columns. Table 2 compares the SMRF structure of NBC and IS models to the other building models. Models S1 to S6 are OMRFs, which are generally noticed in field surveys. The model NBC is designed based on the Nepal building code, and the IS models

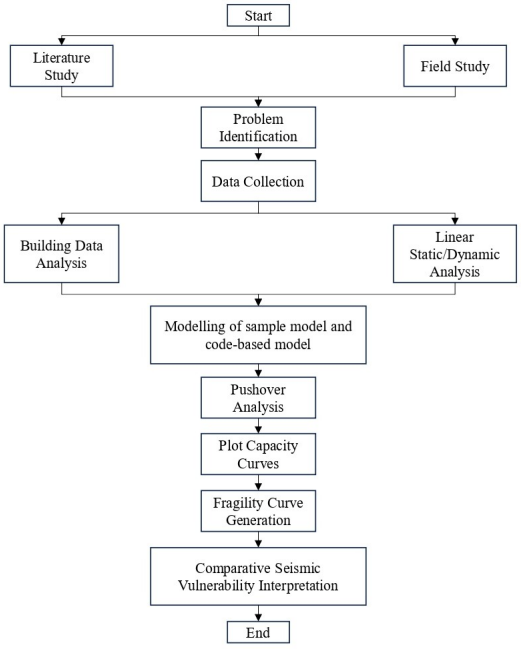

Figure 1 Flowchart of Seismic Vulnerability Assessment Methodology.

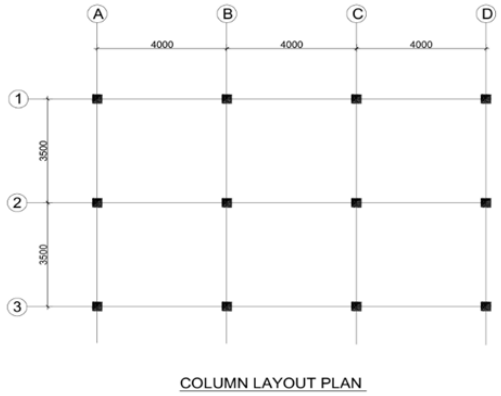

Figure 2 Plan of the building (dimensions in mm).

are designed based on Indian standards. Other models are based on non-engineered buildings observed in Darchula.

The typical characteristics of each building structure studied are presented in sections 2.2 to 2.5.

2.2 Nepal Building Codes (NBCs)

In 2010, the Department of Urban Development and Building Construction published further suggestions for earthquake-resistant building construction in Nepal, with the help of UNDP. This document is based on the National Building Code (NBC) (Mahal and Kathmandu, 2013) and defines the minimum dimensions of columns needed for structures up to three stories.

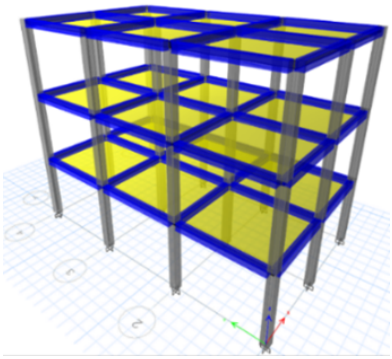

Figure 3 3D view of the RC buildings.

Table 1. Material properties, loads, and seismic parameters of the case study buildings

Material properties		
Grade	concrete	M20
	steel	415 MPa
Modulus of elasticity	concrete	22.36 GPa
	steel	200 MPa
Loads		
Live load on floor level		3 kN/m^2
Live load on roof level		1.5 kN/m^2
Finishing in roof load		1 kN/m^2
Weight of the wall on each floor		11.2 kN/m
Weight of the parapet wall in the roof		4 kN/m
Seismic factor		
Seismic zone according to the Indian standard		V
Zone factor (Z) according to the Indian standard		0.36
Importance factor for all models (I)		1
Type of soil (assumed)		II
Response reduction factor R (SMRF)		5
Response reduction factor R (OMRF)		3

Table 2. Model information for the case study RC buildings

Models	Size of column (mm × mm)	Reinforcement used in column	Tie bar used in column	Size of beam (mm × mm)
NBC	300 ×300	4-12 Ø +4-16 Ø	8 Ø	250 × 300
RUD	350 × 350	8-20 Ø	8 Ø	250 × 380
		8-16 Ø	8 Ø	250 × 355
IS	300 × 300	8-16 Ø	8 Ø	250 × 300
S1	300 × 300	4-12 Ø	6 Ø	230 × 250
S2	300 × 300	4-16 Ø	6 Ø	230 × 250
S3	300 × 300	6-12 Ø	6 Ø	230 × 250
S4	230 × 230	4-12 Ø	6 Ø	230 × 230
S5	230 × 230	6-12 Ø	6 Ø	230 × 250
S6	250 × 230	4-16 Ø	6 Ø	230 × 250

2.3 Newly Revised Building COdes (RUD)

The national building code for Nepal, NBC 205:2024 (DUDBC, 2024), is a RUD guideline for low-rise three-story buildings made of reinforced concrete without masonry infill. The primary objective of this RUD Guideline is to provide practical details and dimensions for various elements in RC-framed and residential buildings up to three stories tall, typically constructed by owner-builders in Nepal, and for popular non-engineered construction practices to meet the basic seismic safety requirements.

2.4 Indian Standards (IS)

The structure was designed by following Indian standard codes for seismic zones, specifically Zone V, which has high earthquake risk. The building's low height and regularity allowed seismic analysis via the seismic coefficient method (IS 1893-2016) (Bureau of Indian Standards, 2016). The columns and beams are designed according to IS 13920:1993 (Bureau of Indian Standards, 1993) for ductile detailing. The IS 875 standard was used to calculate the dead and live load, while the IS 456-2000 standard was used for the load combinations as shown in Table 1.

2.5 Common Constructed Buildings (S1, S2, S3, S4, S5, S6)

This sort of structure reflects the prevailing construction techniques in Darchula, Nepal. Buildings are typically constructed using low-rise RC frames without masonry infill. As urbanization increases and land prices rise, owners often add extra stories to existing buildings without planning for these additional floors or considering seismic safety. As the height increases, high occupancy levels pose a significant risk in urban areas during an earthquake.

In this study, non-engineered RC buildings refer to RC frame structures constructed without formal structural design, typically found in rural and urban areas (Darchula). These buildings are not designed or reviewed by qualified engineers and often fail to meet national as well as Indian seismic code requirements. The models S1 through S6 represent typical field-observed variations in column cross-sectional dimensions and reinforcement ratios (see Table 2), based on detailed surveys conducted in the region. Previous earthquakes in adjacent regions have highlighted the devastating repercussions of such structural collapse, resulting in severe loss of life and extensive property destruction (Poudel and Chaulagain, 2024). The structural and seismic parameters used in this study were derived from field data, national/international codes, and engineering best practices. A summary of the key parameters and their justifications is presented in Table 3.

2.6 Nonlinear Static Analysis Modeling

Nonlinear pushover analysis is a commonly used technique in seismic vulnerability assessment to analyze the structure' s performance under lateral loads, particularly during earthquake events (Prajwal et al., 2017). Numerous guidelines and standards, such as Eurocode 8 (2005) (Tenchini et al., 2016), ATC-40 (1996), and FEMA 356 (2000) (FEMA 356, 2000) emphasize the necessity to comprehend how structures react beyond their elastic limit and encourage the use of nonlinear static processes, such as pushover analysis. Pushover nonlinear static analysis was used to assess the seismic capabilities of the nine buildings. For nonlinear analysis in each model, the finite element method software ETABs (2022) was used.

To assess the seismic performance of the structure, displacement-control pushover analysis is a sophisticated nonlinear static approach (Chopra and Goel, 2002; Dya and Oretaa, 2015). This analysis in ETABS entails applying increasing displacement or lateral displacement until the structure achieves the desired displacement. Nonlinear modeling of the columns and beams was performed. Plastic hinges were assigned at the ends of the beam and column. ETABS allows the selection of predefined hinge properties based on ASCE 41 (ASCE/SEI 41-17, 2017). The analysis is made simpler by using plastic hinges, which assume that inelastic behavior only occurs in these hinges while the rest of the element stays elastic. These hinges represent the deformation-controlled behavior (ductile response) of the element, allowing for large rotations without immediate failure. Flexural hinges are assigned near the ends of columns and beams to simulate the inelastic rotation that occurs during seismic events. For columns, a coupled degree of freedom ($P-M-M$) hinge is defined, accounting for the interaction between axial forces (P) and moments (M) in two directions. For beams, an uncoupled ($M3$) degree of freedom hinge is used, considering only the moment about the strong axis (bending in one direction). Beam-column joints were modeled as rigid connections in ETABS. The study does not explicitly model joint shear failure; however, the effects of poor joint detailing, common in non-engineered RC buildings, were indirectly accounted for through reduced material strength and reinforcement assumptions. In ETABS, plastic hinges can be defined via the auto hinge option, which simplifies the modeling process by automatically assigning hinge properties based on predefined parameters from codes such as ASCE/SEI 41-17 (2017).

In this research, a nonlinear static pushover analysis was carried out using plastic hinges to represent flexural behavior in line with FEMA-356 guidelines. Checks on shear capacity were performed to confirm that structural elements satisfied the minimum shear strength criteria under lateral forces. Nevertheless, shear failure was not explicitly represented in the nonlinear response due to software limitations and scope constraints. This simplification is deemed acceptable for an initial seismic vulnerability assessment but should be improved upon in future studies to more accurately represent potential brittle failure modes.

Table 3. Summary of the modeling parameters and their corresponding sources

Parameter	Value/Range Used	Source/Justification
Column size (non-engineered)	230 mm × 230 mm to 300 mm × 300 mm	Based on field measurements of existing buildings in Darchula
Column size (engineered)	≥300 mm × 300 mm (NBC), 320 mm × 320 mm (RUD)	Nepal National Building Code (NBC 205:2024), and Indian standard IS 456:2016
Reinforcement ratios	0.7% to 1.2%	Field data and code recommendations
Beam size	230 mm × 300 mm to 300 mm × 450 mm	Common practices observed and code minimums
Seismic zone	Zone V	Indian Standard IS 1893
Soil type	Medium to soft soil	Based on site reconnaissance
Load combinations	As per IS 456 guidelines	Standard code-based design practice
Seismic analysis method	Linear static and nonlinear pushover	As per the code and guidelines

3 RESULTS AND DISCUSSION

3.1 Analysis of Survey Data on Building Practices and Seismic Vulnerability

Most of the buildings in rural areas, such as Darchula, fall under the non-engineered category, including adobe, stone, block, and mud structures. These areas are highly vulnerable to seismic events, such as the 2015 Gorkha earthquake (Varum et al., 2018) and the Jajarkot earthquake (Poudel and Chaulagain, 2024), which severely impacted traditionally built homes. However, a large portion of the population continues to rely on non-engineered buildings, especially in remote and economically disadvantaged areas. Buildings with more than 1,000 sq. ft. The plinth area has more than three stories and a structural span greater than 4.5 m, must follow NBC 101 to NBC 114 and NBC 206 to NBC 207 (DUDBC, 1994). Smaller buildings, under 1,000 sq. ft., fewer than three stories, and spans under 4.5 meters, follow thumb rules in NBC 201, 202, and 205, which provide provisions for beam and column dimensions and structural detailing (DUDBC, 2024).

To increase the earthquake resistance of buildings, NBC 205:2070 introduced revisions, including a recommen-

dation that the column's minimum size should be 300 mm × 300 mm for structures up to three stories, with column-to-column spans of less than 4.5 meters. Recently, the new Ready to Use (RUD) code NBC 205: 2024 was introduced for low-rise reinforced concrete buildings for up to 3-story regular buildings. This code introduced a new column size of 320 × 320 mm (minimum Size) and 4-16 Ø+4-12 Ø minimum number of reinforcements in the buildings (DUDBC, 2024). Despite clear guidelines, compliance remains low. The public views the permit process as costly and time-consuming due to fees and taxes. A study of column sizes in 238 buildings revealed that only 43% of the structures followed the recommended column size of 300 mm × 300 mm, whereas approximately 48% of featured columns are smaller than this standard, and 18% of buildings that are taller than two stories have undersized columns, which is due to a lack of awareness of building laws as shown in Figure 4. A survey revealed that many buildings were unregistered or built in compliance with established codes and bylaws during the last six years, highlighting gaps in public knowledge and enforcement.

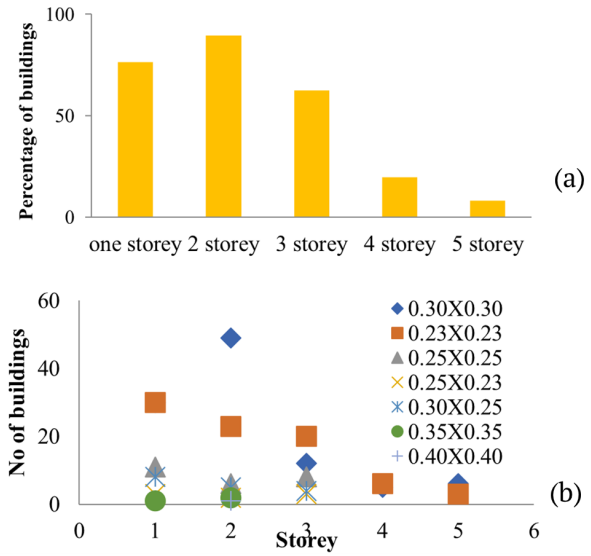

Figure 4 Relationship between the (a) Percentage of RC building data and the number of stories, (b) cross-section of columns based on the number of stories.

In RC buildings, the connection between beams and columns is the most critical part of the design, especially in earthquake-prone areas (Bohara et al., 2025). If these joints are not properly designed to be strong and flexible, the entire building could collapse during a quake. In the 2015 Gorkha earthquake, column-beam joint failure was observed, which was due to insufficient transverse reinforcement and detail (Gautam et al., 2016). In the Mahakali Municipality, many buildings have poorly constructed column-beam joints, where the column and beam joints are not cast together, which weakens the connection.

The data reveals that some buildings consist of small column sections (230 mm × 230 mm) with less than a minimum of 0.8% rebar and almost the same beam section, violating the code rule. This problem is observed in old and new buildings of up to 5 stories, in which some columns are too small and contain less steel than required by the building codes. Insufficient stirrup spacing and weak confinement of the RC section are also observed in the RC buildings in the Mahakali municipality. The beams and columns lack the proper reinforcement during observation and against the MRT Nepal building codes. The detailed requirements for lap-splice, beam, and columns, and the number of main reinforcements are under the requirements. As per the code, the number of longitudinal rebars is limited to more than 16 mm diameter bars ranging from 4 – 8 bars, but it is observed that 10 mm and 12 mm bars are only provided in columns, as shown in Figure 5. Moreover, 6 mm diameter bars are used as a stirrup with a spacing of 0.15 m or more. Some step-back buildings, buildings with open lower stories and infilled brick masonry wall upper stories, resulted in soft stories as shown in Figures 6(a) and (b). About 11% are soft-story buildings, and during several earthquakes, soft-story failure causes building collapse (Gautam et al., 2015; Bohara et al., 2022). The soft-story building's columns are 230 mm × 230 mm and 230 mm × 300 mm in size, having a minimum amount of steel, indicating that the structures are seismically dangerous. In beams, columns, and eventually foundations, the lateral load is not efficiently transferred due to the discontinuity of the load path during earthquakes shown in Figures 6(c) and (d).

Figure 5 (a) No proper anchorage in column-beam joints and stirrup spacing (b), (c), and (d) poor column-beam joint spacing.

Figure 6 (a) Poor column-beam joints, a soft story; (b) poor beam column, soft story, floating columns; (c) Load accumulation in the upper floor; (d) floating columns.

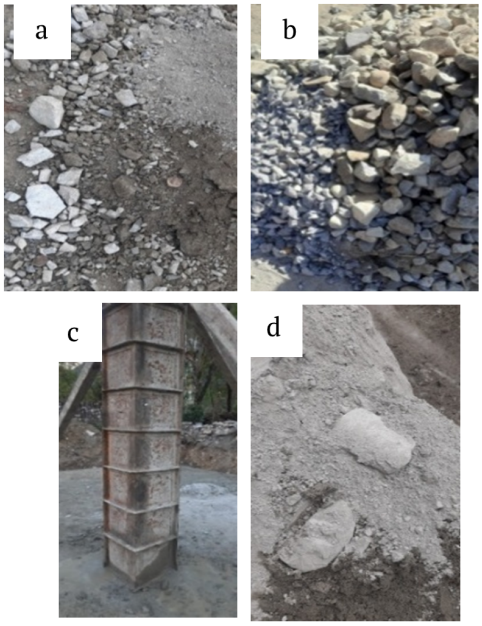

Figure 7 (a) and (b) An improper aggregate size is used. (c) Cement outflow from the lowest section of the formwork. (d) A cement lump has been found at the site.

In hilly areas such as Darchula, there are notable difficulties concerning the quality and accessibility of construction materials, which frequently result in substandard building practices. Whereas excessive filler materials such as sand are incorporated because of the use of incorrectly shaped and oversized coarse aggregates, generally ranging from 40 mm to 70 mm, as illustrated in Figures 7(a) and (b). Additionally, improper mixing techniques, unsuitable water-cement ratios, and inadequate vibration during the construction process lead to problems such as segregation and bleeding of concrete, especially in columns, further jeopardizing structural stability shown in Figures 7(c) and (d). As a result of the honeycombing effects observed in the beams, columns, and slabs, the primary reinforcements are easily visible, which leads to corrosion. Improper covers are observed in the columns, and owing to this visible patching, plaster is applied to the columns to cover them. As seen in Figure 7(c), nearly all of the column's height (more than 1.5 m) is cast in a single stage, causing various types of defects in the columns. As seen in Figure 7(c), the cement used in construction is three months old, demonstrating the inferior quality of the materials.

3.2 Numerical Analysis

3.2.1 Model Mass Participation Ratio, Periods, and Design Base Shear

Table 4 shows the key seismic parameters across multiple models (S1 to S6) compared with codes such as Nepal's NBC, RUD, and IS 1893. According to Indian Standard 1893 (Part I): 2016, the data derived from linear elastic analysis establishes seismic design forces. A structure's global seismic requirements are determined by its fundamental period, mode shape, and design base shear (Bohara, 2021). The first mode periods range from 0.602 to 1.144 sec across different models, showing variability based on structural characteristics such as the height, stiffness, and mass distribution of the structures. Buildings with periods of approximately 0.75 sec – 0.79 sec (NBC, RUD, and IS) might represent typically designed or engineered buildings. Whereas models with longer periods (S4 at 1.144 sec) could indicate non-engineered buildings and more flexible structures, it is due to their low stiffness, resulting from small column sections, poor reinforcement detailing, absence of infill walls. Buildings with longer periods, such as models S4-S6, might require more robust lateral reinforcement to control deflection. Table 4 also shows that all the models achieve high mass participation ratios close to 0.88-0.90 in the first and second modes, which is favorable per IS 1893. For seismic design, IS 1893 recommends ensuring mass participation ratios above 0.85 in the first few modes to capture an adequate dynamic response under seismic loading. The high mass participation values here indicate efficient dynamic response and resonance control in the models. The base shear values were high in models S1, S2, and S3, whereas lower values were observed in models NBC and IS. In linear analysis, it is difficult to understand the strength capacity of buildings. While linear analysis is suitable for preliminary design and compliance with basic code requirements, pushover analysis provides a detailed understanding of the inelastic behavior and true strength of the structure.

Table 4. Summary of the modeling parameters and their corresponding sources

Seismic parameters	Mode/axis	NBC	RUD	IS	S1	S2	S3	S4	S5	S6
Periods of the building models (in Seconds)	1st mode	0.750	0.600	0.757	0.790	0.790	0.790	1.140	1.130	1.020
	2nd mode	0.755	0.601	0.755	0.787	0.787	0.787	1.139	1.131	0.853
	3rd mode	0.665	0.528	0.665	0.700	0.700	0.700	0.999	0.989	0.849
Mass participation ratio	1st mode	0.89	0.88	0.89	0.88	0.88	0.88	0.90	0.90	0.90
	2nd mode	0.89	0.88	0.89	0.88	0.88	0.88	0.90	0.90	0.89
Base shear (kN) of the building models	X-axis	245.8	319.8	245.8	384.1	384.1	384.1	258.2	261.7	291.5
	Y-axis	246.5	320.8	246.5	386.1	386.1	386.1	259.2	262.6	35.8
Ratio of base shear to seismic weight (dead load + reduced live load) (kN)	X-axis	0.065	0.081	0.065	0.103	0.103	0.103	0.071	0.072	0.079
	Y-axis	0.065	0.081	0.065	0.104	0.104	0.104	0.072	0.072	0.096

3.2.2 Capacity Curve and Inter-Story Drift (ISD)

The building capacity curve or pushover curve is an essential tool in seismic analysis, offering insight into how a building responds to lateral loads, particularly in an earthquake scenario. It is essentially a force-displacement plot, where the building' s resistance to lateral loads is plotted against a characteristic lateral displacement, usually the displacement of the roof or other significant points on the structure (Ali and Sanghai, 2021; Bohara and Saha, 2022). This curve typically passes through several key stages, Elastic Range: Initially, the structure behaves elastically, meaning that the deformation is directly proportional to the applied force. Yield Point: At this point, the structure begins to exhibit nonlinear behavior, with some elements, such as beams and columns, forming plastic hinges. Post-yield behavior: After yielding, the structure still resists additional loads, but its stiffness gradually decreases as more plastic hinges form and deformation localizes in certain structural elements. Ultimate capacity: This is the maximum strength the structure can achieve before experiencing significant degradation in load-carrying capacity, possibly leading to structural failure. By transforming the base shear into spectral acceleration (S_a) and the roof displacement into spectral displacement (S_d), the base shear and displacement are converted into spectral coordinates. These changes make it possible to compare the capacity curve and the earthquake response spectrum directly, giving an indication of the seismic demand on the structure at various intensities.

For each X and Y loading direction, the findings of the nonlinear pushover analysis for the examined building models can be seen in Figure 8. In this study, the base shear force of the model RUD building was greater than that of the other models in both the X and Y directions of loading. The results show that the capacity strengths of the RUD and IS models were greater than those of the NBC model. Compared with engineered buildings, other non-engineered buildings have lower strength capacities. The graph illustrates the inter-story drift (ISD%) across different story levels for multiple building models. All the models consistently exhibit a greater ISD at the ground story than at the upper levels, indicating that the ground floor experiences the most lateral deformation under seismic loads, likely due to increased flexibility or a soft story effect. The IS drift rate of change is regular and consistent across the upper stories for all the models, suggesting a uniform distribution of stiffness and controlled deformation throughout the structures above ground level. This consistency across models indicates that all buildings maintain a similar drift pattern, although specific ISD values vary by model, as shown in Figure 9.

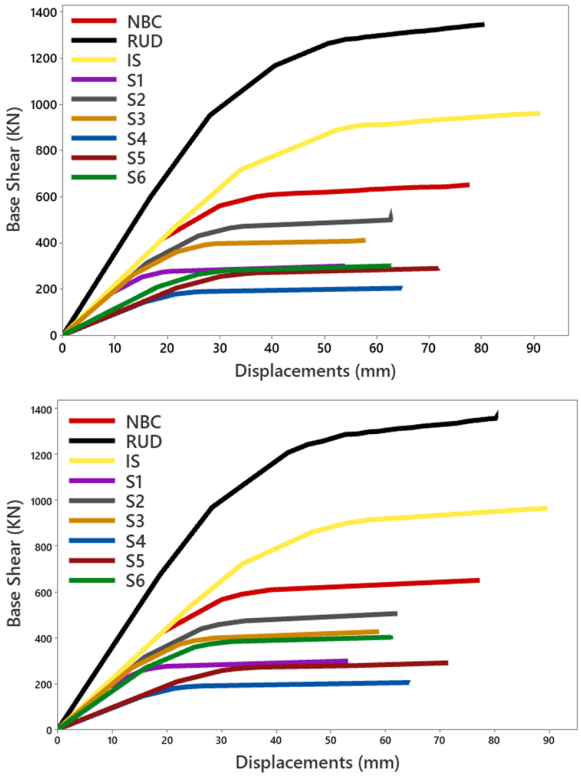

Figure 8 Capacity curves of models in the (a) X-direction and (b) Y-direction) and (b) An improper aggregate size is used. (c) Cement outflow from the lowest section of the formwork. (d) A cement lump has been found at the site.

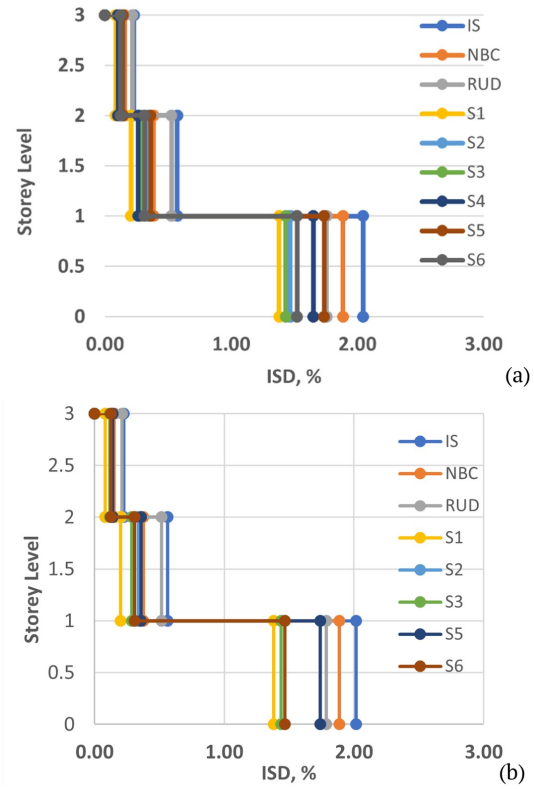

Figure 9 Inter-story drift curves of the models in the (a) X-direction and (b) Y-direction.

3.3 Fragility Analysis

In an earthquake, fragility curves show the likelihood that a building may reach or surpass specific damage levels according to its capacity and seismic demand (Gautam et al., 2021; Chapagain and Chaulagain, 2024). These curves are derived via probabilistic models that consider both the variability in the building capacity and the intensity of ground shaking (Ahmad et al., 2018). The risk-UE methodology provides a standardized approach for generating fragility curves based on extensive empirical and analytical data. HAZUS FEMA (2020) classifies damage into four categories: slight damage, minor cracking, and little or no permanent deformation. Moderate damage involves cracking and minor yielding; extensive damage includes plastic hinge formation and element failure; complete damage indicates collapse or imminent failure of critical components. The damage state thresholds are determined as a function of the spectral displacement (S_d) yielding and ultimate values of the pushover curve after being transformed into acceleration and displacement response spectra (ADRSs).

$$S_{d1} = 0.7\, S_{dy} \quad (1)$$

$$S_{d2} = S_{dy} \quad (2)$$

$$S_{d3} = S_{dy} + 0.25\,(S_{du} - S_{dy}) \quad (3)$$

$$S_{d4} = S_{du} \quad (4)$$

where S_{dy} and S_{du} represent the yielding and ultimate spectral displacement of the idealized capacity curve, respectively. Fragility curves are created by connecting seismic demand (such as PGA or S_d) with structural capacity derived from the capacity curve. The fragility curve is expressed by the following equation:

$$P\left[DS \geq DS_i | D\right] = \Phi\left(\frac{1}{\beta_i} \ln\left(\frac{S_d}{\bar{S}_d}\right)\right) \quad (5)$$

where $P\left[DS \geq DS_i | D\right]$ is the probability that the damage state DS_i is exceeded for a given demand D. D is the seismic demand (typically represented by displacement or drift). S_i is the median capacity of the building corresponding to damage state DS_i. where β_i is the dispersion parameter (standard deviation), which represents the uncertainty in the building's capacity and demand and Φ is the normal distribution function. Each fragility curve corresponds to a different damage state (slight, moderate, extensive, and complete), and the fragility function calculates the likelihood that a building will surpass a specific damage condition given a specific seismic demand. The standard deviation (σ) for each damage state was calculated by fitting a normal cumulative distribution function (CDF) to the probabilities provided in Barbat (Barbat et al., 2008). Table 5 displays spectral displacement values (Sd_1–Sd_4) that indicate average points for various damage states. An optimization process reduced squared errors by comparing observed probabilities to normal CDF values, adjusting σ iteratively while keeping means constant, for each structure and damage state separately.

Table 5. Probabilities for each fragility curve to fit the data (Barbat, Pujades and Lantada, 2008)

Condition	$P_\beta(1)$	$P_\beta(2)$	$P_\beta(3)$	$P_\beta(4)$
$P_\beta(1)$	0.500	0.119	0.012	0.000
$P_\beta(2)$	0.896	0.500	0.135	0.008
$P_\beta(3)$	0.992	0.866	0.500	0.104
$P_\beta(4)$	1.000	0.988	0.881	0.500

Fragility curves are constructed and presented in Figure 10 for all the damage states and structures. The means and standard deviations of the structures are summarized in Table 6.

3.3.1 Discussion and Results of the Fragility Assessment

Table 6 displays the mean and standard deviation values for each damage state, reflecting spectral displacements with a 50% exceedance probability. Increased mean values imply enhanced seismic resistance, acting as vital measures of structural sensitivity among the buildings assessed (Liu et al., 2023; Rc et al., 2025). The fragility curves in Figure 10, combined with the data from Table 6, highlight the significant differences in seismic performance between buildings designed according to modern codes (NBC, RUD, IS) and non-

engineered structures (S1 – S6). Structures designed according to standards (NBC, RUD, and IS) present significantly higher mean values across all damage states than non-engineered buildings do (S1 – S6). For example, for the complete damage state, the mean values for NBC, RUD, and IS are 61.5, 63.1, and 72.1, respectively, whereas for noncompliant structures, the values range between 42.08 (S1) and 55.5 (S5). This highlights the enhanced seismic resilience of engineered buildings, which are better able to withstand seismic demands before sustaining significant damage (Anggraini et al., 2025; Fauzan et al., 2025).

Structures such as S1 and S2 present lower mean values across all damage states, indicating greater fragility. For example, the means for moderate damage are 10.5 for S1 and 17.64 mm for S2, which are significantly lower than those of structures such as S5 and S6. This is primarily due to their reduced flexibility, which makes them more susceptible to higher acceleration demands during seismic events. Buildings, such as S5 and S6, show slightly improved performance, particularly for higher damage states. For example, the mean values for complete damage are 55.5 (S5) and 50.19 (S6), which are greater than those of shorter structures such as S1 (42.08). This improvement is attributed to the greater flexibility of buildings, allowing them to dissipate seismic energy more effectively. However, they remain significantly more fragile than engineered buildings are, primarily because of inadequate detailing and insufficient lateral resistance.

Table 6. Means and standard deviations of each damage state for all the buildings

	Slight		Moderate		Extensive		Complete	
Structure	**mean**	**std**	**mean**	**std**	**mean**	**std**	**mean**	**std**
NBC	14.420	0.007404	20.60	0.008528	30.8250	0.009339	61.50	0.022362
RUD	14.480	0.004912	26.40	0.006613	35.5750	0.008894	63.10	0.022062
IS	21.700	0.006297	31.00	0.007439	41.2750	0.008291	72.10	0.019949
S1	7.350	0.002499	10.50	0.002806	18.3950	0.006522	42.08	0.016883
S2	12.348	0.004196	17.64	0.005499	25.5275	0.006950	49.19	0.017053
S3	10.297	0.003506	14.71	0.004780	22.4075	0.006663	45.50	0.016601
S4	11.172	0.003802	15.96	0.005192	24.9025	0.007668	51.73	0.019247
S5	15.561	0.005306	22.23	0.006483	30.5475	0.007474	55.50	0.018056
S6	13.096	0.004458	18.67	0.005704	26.5500	0.007000	50.19	0.017058

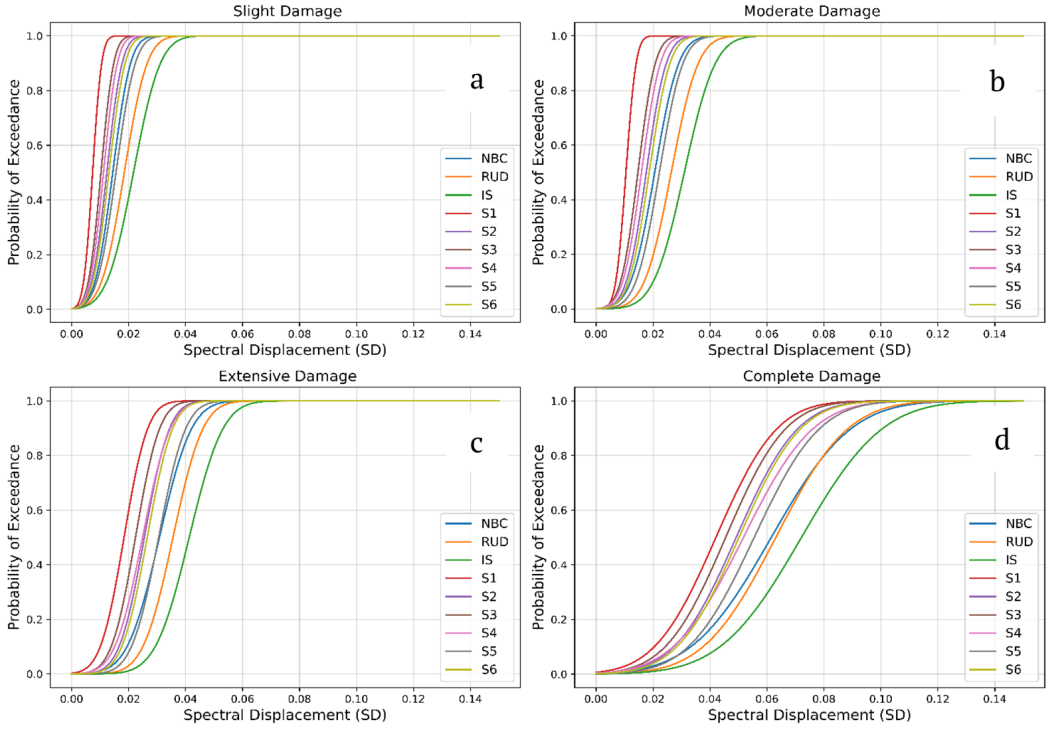

Figure 10 Fragility curves of the studied structures via the RISK-UE LM2 method: a) slight damage, b) moderate damage, c) extensive damage, and d) complete damage.

The standard deviation provides insight into the variability of the damage states. Structures with lower standard deviations (e.g., S1: 0.006522 for extensive damage) show less dispersion in their fragility behavior, suggesting a more consistent response under seismic loading. Conversely, higher standard deviations (e.g., IS: 0.008291 for extensive damage) reflect greater uncertainty, potentially due to differences in design assumptions and construction practices. For all the structures, the mean values increase progressively from slight to complete damage, reflecting the expected increase in the spectral displacement required to reach higher damage states. However, non-engineered buildings consistently present lower mean values for each damage state than their engineered counterparts do (Gautam et al., 2021). This underscores their vulnerability, as they reach critical damage thresholds at much lower levels of seismic demand.

The fragility curves (Figure 10) illustrate a significant difference in seismic behavior between engineered (NBC, RUD, IS) and non-engineered (S1 – S6) reinforced concrete buildings. Engineered structures display higher spectral displacement thresholds across all damage levels, with the IS model demonstrating the highest degree of resilience. On the other hand, non-engineered buildings, especially S1 and S3, exhibit the lowest thresholds for catastrophic damage due to inadequate construction practices and poor detailing. Taller non-engineered structures (S5, S6) perform somewhat better owing to their increased flexibility. These findings underscore the vital impact of construction quality, detailing, and adherence to codes, highlighting the pressing necessity for retrofitting and strict regulation in Darchula, Nepal.

Although fragility curves were developed using a log-normal distribution fitted to spectral displacement values from pushover analysis, this approach simplifies the representation of uncertainty (Nemutlu et al., 2023). The dispersion parameter (β) alone does not fully account for variability in real building performance. Several sources of uncertainty influence the results. First, due to the lack of site-specific ground motion records for Darchula, generalized spectral shapes were used, introducing epistemic uncertainty in seismic input. Second, field observations revealed considerable variability in concrete quality, reinforcement detailing, and column sizes, especially in non-engineered buildings. These contribute to aleatoric uncertainty that is not easily quantifiable. Third, modelling simplifications such as idealized plastic hinges and symmetric layouts do not fully capture the complex behavior of actual buildings. Finally, fitting cumulative distribution functions to damage states assumes smooth transitions that may not reflect observed fragility trends (Rc et al., 2025).

Future studies could improve the reliability of fragility analysis by employing incremental dynamic analysis (IDA), probabilistic Monte Carlo simulations, and sensitivity analyses to better capture input variability and modeling uncertainty.

4 CONCLUSION

The survey and analysis of building practices in rural areas of Darchula, Nepal, reveal significant seismic vulnerabilities in residential and public structures. Most buildings, including recently constructed ones, fail to comply with Nepal's NBC requirements. Key deficiencies include undersized columns, inadequate reinforcement, poor-quality materials, improper beam-column joint construction, and widespread use of non-engineered practices. The analysis of seismic performance for buildings designed according to various standards (NBC, RUD, IS) and non-engineered structures (S1 – S6) reveals significant differences in their vulnerability. Both linear and nonlinear pushover analyses indicate that structures with natural periods between 0.75 and 0.79 seconds exhibit appropriate engineering practices, whereas those with extended periods, like 1.144 seconds for model S4, demonstrate increased flexibility and a demand for enhanced lateral support. Non-engineered models S1, S2, and S3 recorded higher base shear values, while engineered models such as NBC and IS showed comparatively lower values. The nonlinear pushover outcomes indicated that RUD and IS models achieved the greatest base shear capacities, confirming that structures built in compliance with codes exhibit superior strength and resilience in comparison to non-engineered buildings, which are more vulnerable during seismic events. An analysis of inter-story drift (ISD%) revealed that the ground floors consistently undergo the highest levels of deformation due to potential soft-story impacts, while upper floors displayed a more consistent distribution of stiffness. The fragility assessment further highlighted those non-engineered buildings (S1 – S6) are considerably more prone to damage, particularly shorter structures like S1, because of their limited flexibility and insufficient energy dissipation. Additionally, non-engineered models (S5, S6) showed considerable fragility primarily due to inadequate seismic detailing. Conversely, engineered buildings (NBC, RUD, IS) exhibited greater resilience, which can be attributed to improved ductility, lateral strength, and timely reinforcement detailing as required by contemporary seismic codes.

4.1 Recommendation

The findings highlight the urgent necessity of adhering to seismic design regulations and upgrading buildings that do not meet these standards to reduce risks and improve safety in areas susceptible to earthquakes.

Structures that comply with current codes should act as models for enhancing the seismic resilience of future developments. Considering the results, we suggest implementing compulsory seismic evaluations, reinforcing at-risk buildings, ensuring adherence to building codes, offering training for local contractors, and incorporating seismic risk considerations into city planning. These actionable steps are vital for bolstering resilience and minimizing losses associated with earthquakes, especially in high-risk regions like Darchula, where inadequate structural conditions significantly endanger lives and infrastructure.

FUNDING

No funding agency has supported this project.

DISCLAIMER

The authors declare no conflict of interest.

REFERENCES

Ahmad, N., Shahzad, A., Ali, Q., Rizwan, M. and Khan, A. N. (2018), 'Seismic fragility functions for code compliant and non-compliant RC SMRF structures in Pakistan', *Bull Earthq Eng* **16**, 4675–4703.
URL: *https://doi.org/10.1007/s10518-018-0377-x*

Ali, S. and Sanghai, S. S. (2021), 'Seismic vulnerability assessment of reinforced concrete buildings using pushover analysis', *AIP Conference Proceedings* **2417**(1), 020018.
URL: *https://doi.org/10.1063/5.0072814*

Anggraini, G. D., Mase, L. Z., Supriani, F., Misliniyati, R., Amri, K. and Chaiyaput, S. (2025), 'Unveiling Differences in Seismic Response: Comparative Study of Equivalent Linear and Nonlinear Analyses in the Central Coastal Region of Bengkulu, Indonesia', *Journal of the Civil Engineering Forum* **11**(1), 43–56.
URL: *https://doi.org/10.22146/jcef.13849*

ASCE/SEI 41-17 (2017), *Seismic Evaluation and Retrofit of Existing Buildings*, American Society of Civil Engineers.

Barbat, A. H., Pujades, L. G. and Lantada, N. (2008), 'Seismic damage evaluation in urban areas using the capacity spectrum method: Application to Barcelona', *Soil Dynamics and Earthquake Engineering* **28**(10), 851–865.
URL: *https://doi.org/10.1016/j.soildyn.2007.10.006*

Bhagat, S., Samith Buddika, H. A. D., Kumar Adhikari, R., Shrestha, A., Bajracharya, S., Joshi, R., Singh, J., Maharjan, R. and Wijeyewickrema, A. C. (2018), 'Damage to Cultural Heritage Structures and Buildings Due to the 2015 Nepal Gorkha Earthquake', *Journal of Earthquake Engineering* **22**(10), 1861–1881.
URL: *https://doi.org/10.1080/13632469.2017.1309608*

Bohara, B. K. (2021), 'Seismic Response of Hill Side Step-back RC Framed Buildings with Shear Wall and Bracing System', *International Journal of Structural and Construction Engineering* **15**(4), 204–210.

Bohara, B. K. (2023), 'Study of Common Construction Practices and Structural Defects in RC Buildings in Darchula District Far-Western Nepal', *Far Western Review* **1**(2), 117–137.
URL: *https://doi.org/10.3126/fwr.v1i2.62137*

Bohara, B. K., Ganaie, K. H. and Saha, P. (2022), 'Effect of position of steel bracing in L-shape reinforced concrete buildings under lateral loading', *Research on Engineering Structures & Material* **8**(1), 155–177.
URL: *https://doi.org/10.17515/resm2021.295st0519*

Bohara, B. K., Joshi, N. M. and Jagari, S. (2025), 'Impact of inadequate column performance and repair techniques on the seismic performance of RC buildings', *Discover Civil Engineering* **2**(1), 94.
URL: *https://doi.org/10.1007/s44290-025-00253-5*

Bohara, B. K. and Saha, P. (2022), 'Nonlinear behaviour of reinforced concrete moment resisting frame with steel brace', *Research on Engineering Structures and Materials* **8**(4), 835–851.
URL: *https://doi.org/10.17515/resm2022.383st0404*

Bureau of Indian Standards (1993), *IS 13920: Ductile Detailing of Reinforced Concrete Structures Subjected to Seismic Forces – Code of Practice*.

Bureau of Indian Standards (2016), *Indian Standard Criteria for Earthquake Resistant Design of Structures: General Provisions and Buildings (IS 1893: Part 1, 2016)*.

Chapagain, K. and Chaulagain, H. (2024), 'Seismic Fragility Analysis of Existing Old Newari Brick Masonry Building in Pokhara Valley', *Structural Mechanics of Engineering Constructions and Buildings* **20**(2), 120–133.
URL: *https://doi.org/10.22363/1815-5235-2024-20-2-120-133*

Chaulagain, H., Gautam, D. and Rodrigues, H. (2018), Revisiting Major Historical Earthquakes in Nepal: Overview of 1833, 1934, 1980, 1988, 2011, and 2015 Seismic Events, *in* D. Gautam and H. Rodrigues, eds, 'Impacts and Insights of the Gorkha Earthquake', Elsevier, pp. 1–17.
URL: *https://www.sciencedirect.com/science/article/pii/B9780128128084000018*

Chopra, A. K. and Goel, R. K. (2002), 'A modal pushover analysis procedure for estimating seismic demands for buildings', *Earthquake Engineering and Structural Dynamics* **31**(3), 561–582.
URL: *https://doi.org/10.1002/eqe.144*

DUDBC (1994), *Nepal National Building Code NBC 105:2020 – Seismic Design of Buildings in Nepal*, Department of Urban Development and Building Construction. Available at: dudbc.gov.np.

DUDBC (2024), *Nepal National Building Code NBC 205:2024 – Ready-to-use Detailing Guideline for Low Rise Reinforced Concrete Buildings Without Masonry Infill*, Department of Urban Development and Building Construction.

Dya, A. F. C. and Oretaa, A. W. C. (2015), 'Seismic vulnerability assessment of soft story irregular buildings using pushover analysis', *Procedia Engineering* **125**, 925–935.
URL: *https://doi.org/10.1016/j.proeng.2015.11.103*

Fauzan, Jauhari, Z. A., Agista, G. A., Yokota, A. and Putra, M. E. (2025), 'Seismic and Tsunamis Vulnerability Assessment of the Shelter School Building Structure with and without Retrofitting', *Journal of the Civil Engineering Forum* **11**(1), 89–100.
URL: *https://doi.org/10.22146/jcef.13432*

FEMA (2020), *Hazus Earthquake Model Technical Manual Hazus 4.2 SP3*, Federal Emergency Management Agency.

FEMA 356 (2000), *Prestandard and Commentary for the Seismic Rehabilitation of Buildings*, Federal Emergency Management Agency.

Gautam, D., Adhikari, R. and Rupakhety, R. (2021), 'Seismic fragility of structural and non-structural elements of Nepali RC buildings', *Engineering Structures* **232**.
URL: *https://doi.org/10.1016/j.engstruct.2021.111879*

Gautam, D., Bhetwal, K. K., Rodrigues, H., Neupane, P. and Sanada, Y. (2015), Observed Damage Patterns on Buildings during 2015 Gorkha (Nepal) Earthquake, *in* 'Proceedings of the 14th International Symposium on New Technologies for Urban Safety of Mega Cities in Asia', number 14, p. 8.

Gautam, D., Rodrigues, H., Bhetwal, K. K., Neupane, P. and Sanada, Y. (2016), 'Common structural and construction deficiencies of Nepalese buildings', *Innovative Infrastructure Solutions* **1**(1), 1–18.
URL: *https://doi.org/10.1007/s41062-016-0001-3*

Gondaliya, K., Amin, J., Bhaiya, V., Vasanwala, S. and Desai, A. (2025), 'Seismic Vulnerability Assessment of Building Stocks in the Western Zone of Surat-City, Gujarat, India, Using the Capacity Spectrum – Based Method', *Journal of Structural Design and Construction Practice* **30**(1).
URL: *https://doi.org/10.1061/JSDCCC.SCENG-1608*

Liu, W., Zhang, J., Liu, H., Wang, F., Liu, J. and Han, M. (2023), 'Seismic Fragility Analysis of Existing RC Frame Structures Strengthened with the External Self-Centering Substructure', *Buildings* **13**(8).
URL: *https://doi.org/10.3390/buildings13082117*

Mahal, B. and Kathmandu, N. (2013), *Nepal National Building Code: Ready to Use Guideline for Detailings of Low Rise Reinforced Concrete Buildings Without Masonry Infill*. NBC Guideline 2070.

Maharjan, S., Poujol, A., Martin, C., Ameri, G., Baumont, D., Hashemi, K., Benjelloun, Y. and Shible, H. (2023), 'New Probabilistic Seismic Hazard Model for Nepal Himalayas by Integrating Distributed Seismicity and Major Thrust Faults', *Geosciences (Switzerland)* **13**(8).
URL: *https://doi.org/10.3390/geosciences13080220*

Nemutlu, Ö. F., Sari, A. and Balun, B. (2023), 'A Novel Approach to Seismic Vulnerability Assessment of Existing Residential Reinforced Concrete Buildings Stock: A Case Study for Bingöl, Turkey', *Iranian Journal of Science and Technology - Transactions of Civil Engineering* **47**(6), 3609–3625.
URL: *https://doi.org/10.1007/s40996-023-01206-7*

Parajuli, H. R., Bhusal, B. and Paudel, S. (2021), 'Seismic zonation of Nepal using probabilistic seismic hazard analysis', *Arabian Journal of Geosciences* **14**(20).
URL: *https://doi.org/10.1007/s12517-021-08475-4*

Poudel, H. R. and Chaulagain, H. (2024), 'The Jajarkot Earthquake: Revealed the Vulnerability of Load Bearing Structures in Western Nepal', *Himalayan Journal of Applied Science and Engineering* **5**(1), 1–22.
URL: *https://doi.org/10.3126/hijase.v5i1.68334*

Prajwal, T. P., Parvez, I. A. and Kamath, K. (2017), 'Nonlinear Analysis of Irregular Buildings Considering the Direction of Seismic Waves', *Materials Today: Proceedings* **4**(9), 9828–9832.
URL: *https://doi.org/10.1016/j.matpr.2017.06.275*

Rc, B., Shirkol, A. I., Gondaliya, K. and Biradar, B. B. (2025), 'Seismic Performance and Fragility Assessment of RC Frame Buildings Equipped with Yielding Brace Systems Using NSPA and IDA', *Journal of Structural Design and Construction Practice* **30**(4), 04025065.
URL: *https://doi.org/10.1061/JSDCCC.SCENG-1726*

Tenchini, A., D'Aniello, M., Rebelo, C., Landolfo, R., Silva, L. S. and Lima, L. (2016), 'High strength steel in chevron concentrically braced frames designed according to Eurocode 8', *Engineering Structures* **124**, 167–185.
URL: *https://doi.org/10.1016/j.engstruct.2016.06.001*

Varum, H., Dumaru, R., Furtado, A., Barbosa, A. R., Gautam, D. and Rodrigues, H. (2018), 'Seismic performance of buildings in Nepal after the Gorkha earthquake', *Impacts and Insights of the Gorkha Earthquake* pp. 47–63.
URL: *https://doi.org/10.1016/B978-0-12-812808-4.00003-1*